Rotation Invariant Finger Vein Recognition

Bernhard Prommegger and Andreas Uhl
University of Salzburg
Jakob-Haringer-Str. 2, 5020 Salzburg, AUSTRIA
{bprommeg, uhl}@cs.sbg.ac.at

Abstract

Finger vein recognition deals with the identification of subjects based on its venous pattern within the fingers. The majority of the scanner devices capture a single finger from the palmar side using light transmission. Some of them are equipped with a contact surface or other structures to support in finger placement. However, these means are not able to prevent all possible types of finger misplacements, in particular longitudinal finger rotation can not be averted. It has been shown that this type of deformation causes severe problems to finger vein recognition systems. This paper proposes two new methods in which finger vein images from different perspectives are captured during enrolment and, but only one during authentication. In the first method, the authentication image is compared to all enrolment images, whereas in the second method they are linked together to form a perspective cumulative finger vein template. As the enrolled finger vein images depict the vein structure of a larger range of the finger, the longitudinal positioning of the finger during the acquisition for the biometric recognition is less critical. The experimental results confirm the applicability especially of the first approach.

1. Introduction

Vascular pattern based biometric systems, commonly denoted as vein biometrics, offer several advantages over other well-established biometric recognition systems. In particular, hand and finger vein systems have become a serious alternative to fingerprint based ones for several applications. Vein based systems use the structure of the blood vessels inside the human body, which becomes visible under near-infrared (NIR) light. As the vein structure is located inside the human body, it is resistant to abrasion and external influences on the skin. Furthermore, a lifeness detection to detect presentation attacks can be performed easily [4].

The performance of finger vein recognition systems suffers from different internal and external factors. Internal factors include the design and configuration of the sensor itself, especially the NIR light source and the camera module. External factors include environmental conditions (e.g. temperature and humidity) and deformations due to misplacement of the finger, typically including shifts, tilt, bending and longitudinal rotation.

Performance degradations caused by various types of finger misplacement are not new and have been addressed in several publications. The need for a robust finger vein image normalisation has already been mentioned by Kumar and Zhou in 2012 [4]. Chen *et al*. [1] state that deformation correction can be done either during pre-processing, feature extraction or comparison. Moreover, the physical design of the sensor can help to avoid misplacements of the finger. In [12] the authors showed, that longitudinal finger rotation has a severe influence on the performance of a finger vein recognition system. There are several approaches that try to reduce the influence of these issues during the processing of the vein patterns. Kumar and Zhou [4] introduced a finger alignment based on the finger boundary to overcome finger translation and rotation. Lee *et al*. [5] proposed a system utilizing a minutia based alignment together with local binary patterns as feature extraction method. Huang *et al*. [2] improved the resistance against longitudinal rotation by applying an elliptic pattern normalization to the input images. Matsuda *et al*. [8] proposed a feature-point based recognition system introducing a finger-shape model and a non-rigid registration method. Yang *et al*. [16] introduced a finger vein recognition framework including an anatomy structure analysis based vein extraction algorithm and integration matching strategy. Chen *et al*. [1] detects different types of finger deformation by analysing the shape of the finger and corrects them using linear and non-linear transformations. Prommegger *et al*. [11] proposed a method that applies a rotation correction on the enrolled templates in both directions using a pre-defined angle for additional comparisons combined with score level fusion. Besides these software based solutions, there are some hardware-based ones which aim to prevent finger misplacements in the first place, during acquisition, rather than correcting them afterwards. Kauba *et al*. [3] presented a finger vein

scanner that requires the subject to place the fingers in a flat, aligned position on a finger shaped guiding surface. This reduces finger misplacements to a minimum. Problems resulting from finger misplacements will receive more attention in the future as finger vein systems evolve towards contact-less operation.

The main contribution of this work is the analysis of two novel rotation invariant finger vein recognition methods and the provision of two new data sets that are designed to allow a thorough analysis of the robustness of finger vein recognition systems against longitudinal finger rotation. Both methods aim to improve the recognition performance by enrolling multiple finger vein images from different perspectives and compare them, just as in current system, against a single sample acquired during authentication. This results in a more complex and expensive enrolment device, whereas the capturing device for authentication remains inexpensive. The first method, multi-perspective enrolment (MPE), uses the acquired enrolment perspectives after applying circular pattern normalization (CPN), the second one combines the different perspectives to form a perspective cumulative finger vein template (PCT). The experiments are carried out using the *PLUSVein finger rotation data set* (PLUSVein-FR) [13]. To show the effectiveness of the proposed approaches, their recognition results are compared to the results of other methods, that claim to be robust against longitudinal finger rotation, utilizing the new data sets.

The rest of this paper is organized as follows: Longitudinal finger rotation and its problems caused for finger vein recognition systems are described in more detail in section 2. Section 3 explains the MPE method and section 4 all details of the generation of the PCT, respectively. The experimental set-up together with its results are described in section 6. Section 7 concludes the paper along with an outlook on future work.

2. Longitudinal Finger Rotation

Typically, finger vein scanners are designed to acquire only a single finger at a time. Different types of finger misplacement can easily occur with these scanners and pose a severe problem. Figure 1 shows the orientations of the x, y and z axis with respect to the finger. The different types of finger misplacement include planar shifts and rotation in the xy-plane, shifts of the finger in z-direction (distance to the camera, scaling), finger bending, finger tilt (finger tip and root are not in the same xy-plane) and longitudinal finger rotation around the y-axis. As described in [12], the influence of some of these problematic misplacements can be reduced or even prevented completely during acquisition by adding support structures for finger positioning or a correction during pre-processing, feature extraction or comparison. Almost all currently available sensors use such support structures, but most of them still do not prevent a rotation around

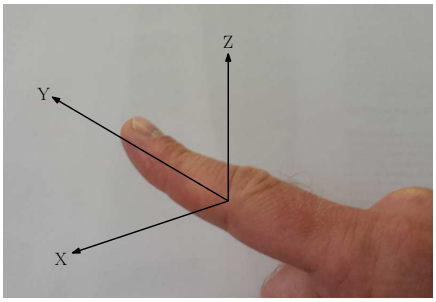

Figure 1. Definition of the axes of a finger in a three-dimensional space (originally published in [11])

the y-axis (longitudinal finger rotation). Thus, longitudinal finger rotation cannot be ruled out and poses a severe problem to finger vein recognition systems.

The captured vein structure is a projection of the vessel structure in the 3D space onto a 2D plane. If the finger is rotated along its longitudinal axis, the vein pattern is deformed according to a non-linear transformation. Figure 2 shows the effect of longitudinal finger rotation on the vein pattern. The finger cross section (top row) is rotated from -30° to +30°. As a result of the rotation the projected pattern of the veins (bottom row) changes as well. Depending on the relative position of the veins to each other and the rotation angle, some of the captured veins might merge into a single one. The vein structures of -30° (left), 0° (middle) and 30° (right) are completely different. Widely used vein recognition schemes can handle such deformations only to a certain extent [12]. If the deformations caused by the longitudinal rotation are corrected, the negative effect can be reduced but not completely prevented [11].

3. Multi-Perspective Enrolment

MPE requires the acquisition of multiple perspectives during enrolment. The acquisition angles of the different perspectives are linearly spaced over the desired acquisition range. For authentication, only a single perspective is acquired and compared to all enrolment samples together with a maximum rule score level fusion. As shown in [11], elliptic pattern normalization (EPN) [2] increases the robustness against longitudinal finger rotation. EPN is based on the hypothesis, that the cross section of a finger approximately resembles an ellipsis and that the veins which are captured by the finger vein scanner are located close to the finger surface. The normalization essentially corresponds to a rolling of the finger, which reduces the non-linear deformation of the vein structure across the entire width of the finger. After this correction is applied, a horizontal shift of the images during comparison corresponds to a rotation of the finger. The elliptic shape normalization proposed by Huang *et al.* holds only true for the palmar and dorsal perspect-

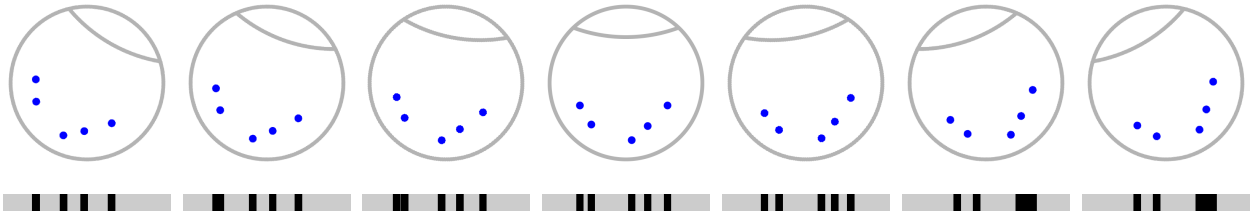

Figure 2. Longitudinal finger rotation principle: a schematic finger cross section showing five veins (blue dots) rotated from -30° (left) to +30° (right) in 10° steps. The projection (bottom row) of the vein pattern is different depending on the rotation angle according to a non-linear transformation (originally published in [12]).

ive. For other perspectives, the resulting shape is different. Therefore, the estimation of the fingers' cross section shape was changed to a circle, resulting in a circular pattern normalization (CPN).

There are already capturing devices available, that are capable of acquiring multi-perspective finger vein images. Prommegger *et al*. [13] proposed a multi-perspective finger vein scanner that acquires a video of the vein structure all around the finger (360°). Veldhuis *et al*. [15] presented a capture device, that acquires images from three perspectives.

4. Perspective Cumulative Finger Vein Templates

As for MPE, also PCT requires the enrolment of finger vein images from multiple perspectives. Again, the rotation angles of the captured samples are spread linearly over the desired acquisition range and are normalized using CPN. Next, the vein pattern is extracted and the single templates are combined to one large cumulative template as following: (1) To suppress unwanted artefacts on the finger edges, some pixels are cut off from both sides. (2) The vein templates are combined together where their overlap reaches the highest correlation. The correlation is calculated as described in [9]. (3) For the first and the last image, the cut-off border is added again after all perspectives have been combined with each other.

During recognition, just as with existing systems, only one perspective is captured and compared to the generated PCT. This comparison is done using a correlation measure, calculated between the PCT and in x- and y-direction shifted and rotated versions of the probe image as described in [9]. The shift is executed over the entire height, which corresponds to the desired angular acquisition range, of the PCT.

During extraction of the vein structure, other details, e.g. skin folds, wrinkles, hair or other texture, are recognized. These distortions can be seen as noise in the vein pattern of the feature image which impede the PCT generation. In order to obtain satisfactory PCTs, these distortions must be reduced to a minimum. Therefore, the level of detail during feature extraction (compared to the level of detail used for other methods) is reduced by smoothing the input image.

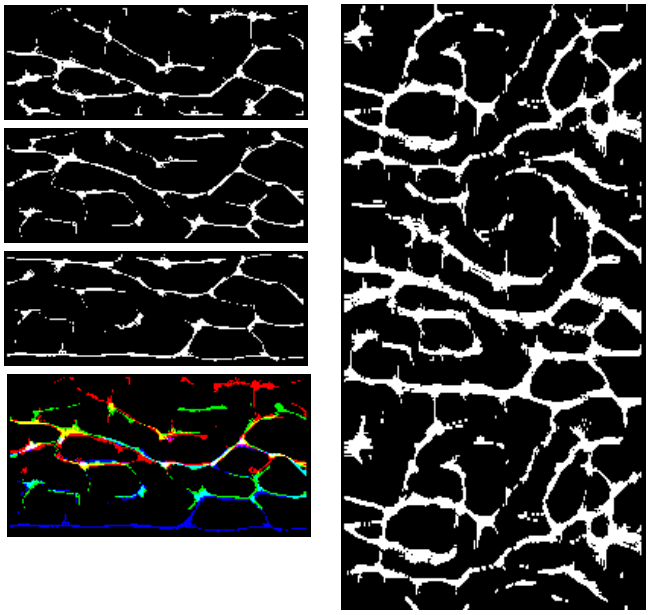

Figure 3. Example of an PCT. Left: single perspectives (rotation angle 30°) and the combined image of the three samples. Right: a PCT on the range of 360°.

Figure 3 shows such a PCT. On the left side there are three samples of finger vein templates with a rotation distance of 30°. The forth row is the combined image of the three samples. The red colour corresponds to the vein pattern of the first image, green to the 2nd one and blue to the third one, respectively. The right side shows the PCT of a finger in the full range of 360° generated with images acquired in a rotational distance of 15°.

Advantages of PCT compared to MBE are the reduced template size and a potential for a lower comparison runtime. The runtime improvement can be achieved by less horizontal shifts applied during the execution of the Miura matcher and the omission of the fusion step.

For a ROI of height h, which corresponds to the estim-

ated diameter of the finger, and length l, n enrolled templates (normalized with CPN) have a total height of

$$h_{MPE} = n \cdot \frac{h \cdot \pi}{2} \tag{1}$$

The PCT height for an angular range of φ is the arc length of φ plus the non-overlapping border of the first and last perspective

$$h_{PCT} = \left(\frac{\varphi}{360} + 2 \cdot \frac{\varphi}{n \cdot 360}\right) \cdot h \cdot \pi = \frac{n+2}{n} \cdot \frac{\varphi}{360} \cdot h \cdot \pi \tag{2}$$

For an enrolment of the whole finger ($\varphi = 360°$) with an angular distance of 30° between the acquired perspectives ($n = 12$), the template size is reduced by factor 5.

The number of horizontal shifts during comparison is related to the size of the templates and the configured shift of the Miura matcher. The shifts for MPE are

$$S_{MPE} = n \cdot (2 \cdot h_{shift} + 1) \tag{3}$$

where h_{shift} is the number of pixels shifted up and down during a comparison. The experiments performed in section 6 showed that a good estimation for h_{shift} is

$$h_{shift} = 2 \cdot \frac{\varphi}{n \cdot 360} \cdot h \tag{4}$$

For PCT, the probe template is shifted over the arc length φ.

$$S_{PCT} = \frac{\varphi}{360} \cdot h \cdot \pi \tag{5}$$

For the above scenario (360°, 12 perspectives), that leads to an reduction of the horizontal shifts by 30%.

5. Performance Validation Data Set

In order to be able to test the robustness of a recognition scheme against longitudinal finger rotation, data sets that depict realistic scenarios regarding finger rotation are needed. Such data sets must satisfy the following characteristics: (1) The data set needs to provide finger vein images from perspectives spread over the desired range. (2) The distribution of the rotation angles must follow the characteristics of the desired scenario. (3) It needs to contain enough longitudinal rotation in order that a rotation compensation is useful. (4) Ideally, also the rotation angles of the different samples are known.

Currently, there exists no publicly available data set that fulfills these properties. Therefore, two new data sets are generated from the publicly available subset (±45° around the palmar view) of the PLUSVein-FR. The first data set, PLUSVein-FR-ED, contains vein images whose rotation angles are equally distributed over the entire range of ±45°. It corresponds to the unconstrained placement of the finger in a contact-less acquisition system. The rotation angles of the second data set, PLUSVein-FR-ND, are normally distributed. This data set models a realistic real world scenario

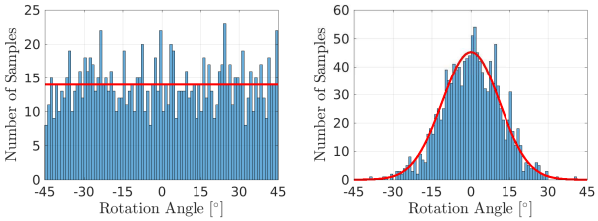

Figure 4. Distribution of rotation angles in the subsets. Left: PLUSVein-FR-ED, right: PLUSVein-FR-ND.

of a classical unsupervised single perspective acquisition system. Prommegger *et al*. estimated the rotation angles of different finger vein data sets in [14]. The SDUMLA-HMT [17] exhibited the highest degree of finger rotation with rotation angles up to 45° ($\sigma = 10.6°$). This standard deviation was used for the generation of the PLUSVein-FR-ND. The distributions of the rotation angles of the two subsets are depicted in Fig. 4. Both data sets are available for download on http://wavelab.at/sources/Prommegger19d.

6. Experiments

In the first part of the experiments, the performance of the proposed methods, MPE and PCT, all around the finger (360°) is analysed using perspectives of the PLUSVein-FR data set in steps of 5°, leading to 73 different perspectives (0° and 360° are acquired separately). Every perspective is considered as a separate data set. The template generation is done in the feature space utilizing MC features [10]. To determine the number of perspectives needed during enrolment, different rotational distances between the used perspective are tested (15°, 30° and 45°). Furthermore, to verify the effectiveness of the proposed methods, in the second part of the experiments both approaches are applied on the two introduced data sets, PLUSVein-FR-ED and PLUSVein-FR-ND, and compared to other finger recognition schemes that are tolerant against longitudinal finger rotation. The necessary enrolment samples are taken from the publicly available ±45° subset of the PLUSVein-FR.

6.1. Recognition Tool Chain

The finger vein recognition tool-chain consists of the following components: (1) For *finger region detection* and *finger alignment* an implementation that is based on [6] is used. (2) The *ROI extraction* differs from [6]: instad of cutting out a defined rectangle within the finger, similar to [2], a normalization of the finger to a fixed width is applied. (3) To improve the visibility of the vein pattern *Circular Gabor Filter* (CGF) [18] and simple *CLAHE* (local histogram equalisation) [19] are used during *pre-processing*. (4) As *feature extraction* method the well-established vein-pattern based *Maximum Curvature* method [10] is employed. (5) The *comparison* of the binary feature images is done us-

ing a correlation measure, calculated between the input images and in x- and y-direction shifted and rotated versions of the reference image as described in [9]. An implementation of the recognition tool-chain is available for download on http://wavelab.at/sources/Prommegger19d.

6.2. Experimental Protocol

For the experiments, the data sets are split into two subsets, one for enrolment and one for authentication. The enrolment subset contains two samples, the one for authentication three. To quantify the performance, the EER, the FMR100 (the lowest FNMR for FMR $\leq 1\%$), the FMR1000 (the lowest FNMR for FMR $\leq 0{,}1\%$) as well as the ZeroFMR (the lowest FNMR for FMR = 0%) are used. For the evaluation, the experiments follow the test protocol of the FVC2004 [7]: For calculating the genuine scores, all possible genuine comparisons are performed, which are $63 \cdot 4 \cdot 3 \cdot 2 = 1512$ matches. For calculating the impostor scores, only the first image of a finger is compared against the first image of all other fingers, resulting in $(63 \cdot 4) \cdot (63 \cdot 4 - 1) = 63252$ matches, so together 64764 matches in total.

As a reference for the quantification of MPE and PCT, the intra-perspective performance of all 73 perspectives, without applying any rotation compensation methods and by applying CPN, is evaluated. For this calculations every perspective is considered as its own data set, which implies, that every perspective is its own independent classical single perspective recognition system, where enrolment and probe image are acquired from the same perspective. Although the results are presented together, they are completely independent from each other. Rotational differences between the enrolment and probe sample would be subject to the same degradations as presented in [11]. Therefore, no rotational invariance can be concluded from the presentation of the intra-perspective results. As MPE and PCT aim to generate rotation invariant recognition results for a single finger vein image acquired from any perspective during authentication, results close to or even better than the intra-perspective results without rotation correction can be considered as good performance.

To quantify the decrease in performance of a method, the relative performance degradation (RPD), which is calculated as stated in equation (6), is used:

$$RPD = \frac{EER_x - EER_{ref}}{EER_{ref}}. \tag{6}$$

EER_{ref} is the EER of the reference data set and EER_x the EER of the evaluated data set. A RPD of 0 means no change in performance, a RPD of 1 corresponds to an EER increase to its doubled value. For a negative RPD, the performance increased. For the evaluation of the performance increase due to rotation correction, the relative performance increase

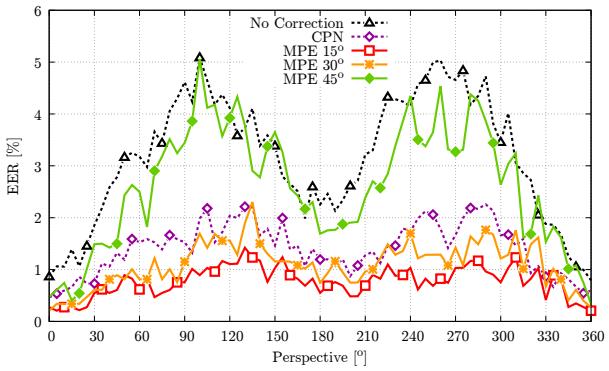

Figure 5. Recognition performance (EER): in-perspective vs MPE comparisons

(RPI) as in equation (7) is calculated:

$$RPI = \frac{EER_{ref} - EER_x}{EER_x}. \tag{7}$$

Again, EER_{ref} is the EER of the reference data set and EER_x the EER of the evaluated data set. A RPI of 0 means no change in the performance, a RPI of 1 corresponds to a drop in the EER to half of its value. For a negative RPI, the performance decreased. All values are given in percentage terms, e.g. 2.35 means 2.35%.

6.3. Results

6.3.1 Multi-Perspective Enrolment

For MPE, three different enrolment scenarios with different distances between the acquired samples are evaluated ($15° \rightarrow 24$ perspectives, $30° \rightarrow 12$ and $45° \rightarrow 8$). Each of the 73 perspectives provided by PLUSVein-FR is compared against all enrolled samples. To get the final score, a simple maximum score level fusion is applied. The trend of the resulting EERs are depicted in Figure 5. Additionally to MPE, also the intra perspective performance results for applying no correction and CPN are visualized. The performance of both methods show the same trend, just at different EER levels: The best performance results are obtained in the palmar (0°) region followed by the dorsal (180°) region. The perspectives inbetween show inferior results, achieving the worst results around 90° and 270°. CPN outperforms no correction over the whole range in average by a factor 2, which corresponds to an RPI of 100%. As expected, the results of the MPE scenarios depend directly on the number of enrolment perspectives: the less the cameras are rotated away from each other, the better the resulting recognition accuracy is. MPE 15° achieves the overall best results. It's EER values are between 0.2 and 1.4% for all perspectives all around the finger, which corresponds to RPIs between 25% and 250%, followed by MPE 30° and MPE 45°. MPE 15° and MPE 30° even outperform the intra per-

Perspective	Method	EER (CI)	FMR100	FMR1000	ZeroFMR	RPD	RPI
0°	No Correction	0.87 (± 0.23)	0.86	1.39	3.71	-	-
	CPN	0.46 (± 0.17)	0.46	0.53	1.19	-	86.8
	MPE 15°	0.27 (± 0.13)	0.28	0.28	0.48	-	215.9
	MPE 30°	0.20 (± 0.11)	0.20	0.27	0.68	-	324.7
	MPE 45°	0.47 (± 0.17)	0.47	0.68	1.56	-	82.9
	PCT 15°	4.25 (± 0.50)	7.08	12.65	35.83	391.1	-
	PCT 30°	4.76 (± 0.53)	7.80	14.71	35.93	449.1	-
	PCT 45°	6.51 (± 0.61)	10.69	17.52	31.19	651.9	-
60°	No Correction	3.18 (± 0.43)	4.70	9.34	30.13	-	-
	CPN	1.53 (± 0.30)	1.66	2.98	7.68	-	108.4
	MPE 15°	0.62 (± 0.20)	0.62	1.24	1.99	-	415.2
	MPE 30°	0.81 (± 0.22)	0.81	1.69	3.99	-	291.6
	MPE 45°	2.50 (± 0.39)	3.11	5.95	13.31	-	27.2
	PCT 15°	5.84 (± 0.58)	11.68	20.54	35.85	83.7	-
	PCT 30°	5.28 (± 0.55)	9.34	16.72	32.97	66.2	-
	PCT 45°	8.11 (± 0.67)	16.28	26.62	53.58	155.2	-
120°	No Correction	4.11 (± 0.49)	5.97	10.01	17.57	-	-
	CPN	2.04 (± 0.35)	2.59	4.18	16.05	-	101.8
	MPE 15°	1.11 (± 0.26)	1.31	2.13	4.61	-	272.3
	MPE 30°	1.56 (± 0.31)	1.63	2.58	12.81	-	163.7
	MPE 45°	3.92 (± 0.48)	5.07	8.66	24.22	-	4.9
	PCT 15°	7.08 (± 0.64)	13.34	25.38	49.38	72.1	-
	PCT 30°	8.34 (± 0.68)	15.32	25.90	44.81	102.8	-
	PCT 45°	11.50 (± 0.79)	23.75	35.86	61.43	179.6	-
180°	No Correction	2.26 (± 0.36)	3.06	5.58	9.30	-	-
	CPN	1.19 (± 0.27)	1.20	2.26	5.25	-	89.1
	MPE 15°	0.55 (± 0.18)	0.48	1.31	3.58	-	310.4
	MPE 30°	0.74 (± 0.21)	0.68	1.63	3.32	-	203.2
	MPE 45°	1.69 (± 0.32)	1.96	3.45	6.90	-	33.6
	PCT 15°	3.37 (± 0.45)	4.40	9.22	15.61	49.1	-
	PCT 30°	4.34 (± 0.50)	5.83	10.17	21.02	92.2	-
	PCT 45°	4.86 (± 0.53)	7.31	11.43	22.60	115.0	-

Table 1. Performance results for evaluation in-perspectiv analysis, MPE and PCT in steps of 45°. RPD and RPI are calculated with respect to *No Correction*

spective CPN results. The performance of MPE 45° is just below the inter perspective comparisons without any correction. Table 1 holds the performance results for selected perspectives. All performance results can be downloaded at http://wavelab.at/sources/Prommegger19d.

6.3.2 Perspective Cumulative Finger Vein Templates

As for MPE, also for PCT three different enrolment scenarios with rotation distances of 15°, 30° and 45° between the acquired perspectives are evaluated. Again, all 73 perspectives are compared against the generated PCT. The trend of the resulting EERs are visualized inf Figure 6. All three methods perform worse than the intra perspective comparisons without any rotation compensation. The course of the PCT curves is relatively even. This also applies to those perspectives for which no enrolment samples have been acquired. Applying PCT 15° results in a RPD between 50% and 400%, PCT 30° between 60% and 450% and PCT 45° between 100% and 650%, respectively. The prominent jump at 180° is due to the generation of the template. It was generated from -180° to +180°. As a result of this, the template contains more information from this perspective as also the border, which was cut off during the template generation, is added to the PCT. The overall inferior results can be explained by the fact, that, as described in section 4, the level of detail had to be reduced in order to achieve satisfactory results when combining the single perspective templates to the cumulative template. Again, table 1 holds the results for selected perspectives.

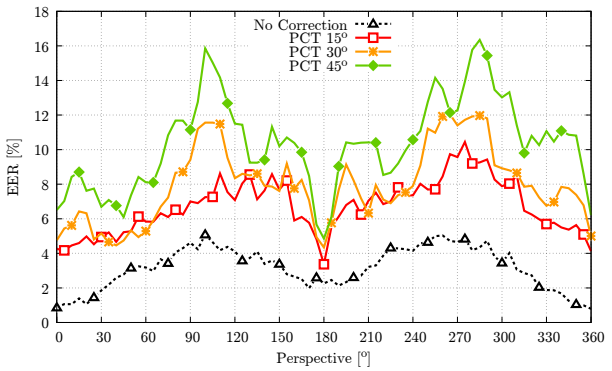

Figure 6. Recognition performance (EER): in-perspective vs PCT comparisons

6.3.3 Performance Validation

For the validation of the performance of the proposed methods, they are compared to well known recognition schemes, that are tolerant against longitudinal finger rotation, namely a rotation compensation using the information of the rotation angle provided by the data set (known angle method) [11], EPN [2], CPN and a method that compensates the rotational deformations without the knowledge of the actual rotation angle by applying a rotation correction in both directions using a pre-defined angle combined with score level fusion (fixed angle correction) [11]. Additionally, the performance of the unmodified data set is stated as a reference. The data sets used for validation are the data sets described in section 5 (PLUSVein-FR-ED and PLUSVein-FR-ND). The validation includes four different MPE scenarios: a two camera version including enrolment cameras positioned $\pm 20°$ from the palmar view (0°), 3 cameras ($\pm 30°$ and 0°), a 4 camera setting ($\pm 45°$ in steps of 30°) and a 7 camera setting ($\pm 45°$ in steps of 15°). The combined templates are again generated for camera distances of 15°, 30° and 45°. The vein images necessary for the MPE scenarios and for the generation of the PCTs are taken from the publicly available *PLUSVein-FR $\pm 45°$ sub set*.

Note that all rotation compensation schemes but MPE and PCT, only acquire a single perspective for enrolment and authentication. As a result of this, they are only tolerant against longitudinal finger rotation to a certain extent ($< \pm 30°$, [11]). MPE and PCT acquire multiple perspectives during enrolment and use this information for authentication against a single perspective. The comparison carried out in this section analyses the performance only in a limited range ($\pm 45°$) in which also single perspective enrolment methods can show a reasonable performance. As shown in the experiments, MPE and PCT are invariant against longitudinal finger rotation all around the finger. Nevertheless, these experiments give a good indication of the strengths (MPE) and weaknesses (PCT) of the proposed approaches.

The results for both data sets are listed in table 2. As mentioned in section 5, the PLUSVein-FR-ED contains finger vein images with rotation angles that are equally distributed in the range of $\pm 45°$. Therefore, the rotation distances between two samples of the same finger might be high. The maximum rotation angle of two samples of the same finger is 89°. This fact is also reflected in the recognition results of the different recognition schemes. Applying only horizontal and vertical shifts (Miura matcher [9]) cannot compensate this rotation. As a result of this, the resulting EER of 21.63% is high. Applying different schemes to increase the robustness against longitudinal finger rotation improves the Performance. EPN improves the performance to an EER of 15.87%, CPN to 15.34% and the fixed angle approach to 5.24%, respectively. As the data set also provides the rotation angle of the samples, it is possible to apply an exact rotation compensation, which improves the EER to 5.44%. The results of the MPE scenarios and the PCT setings are superior even to the exact rotation compensation. This is reasonable: due to the enrolment process, where more than one perspective is aquired for MBE and PCT, they hold more information of the vein pattern of the finger than a single perspective enrolment. Additionally, rotating the finger vein samples into their correct position using the provided rotation angle results in areas of the ROI, that contain no vein information (areas, where no vein information is present are filled with the average grey level of the image). Higher rotation angles result in larger ROI regions without vein information. In case of big distances in the rotation angles, this has a negative effect on the score of the Miura matcher. Fig. 7 shows two samples with a large rotational difference. The left side is rotated 45° to the left, the right one 45° to the right. The unmodified ROI images in the top row show a big difference between the pattern of both images. In the bottom row, which depicts the rotation corrected versions of the images, the vein structure is more similar. Both images hold quite a large region without any vein information. As the same region in the other sample contains vein information, the comparison score is reduced. When applying MPE or comparing to PCT, the samples are not rotated and this effect does not occur. The best results for MPE is achieved in the 7 camera scenario with an EER of 0.33%. The best PCT result with an EER of 3.00% is achieved when the rotational difference between the enrolment perspectives is 15°. This corresponds to an RPI of 6379% for MPE and 620% for PCT compared to the performance on the original data set.

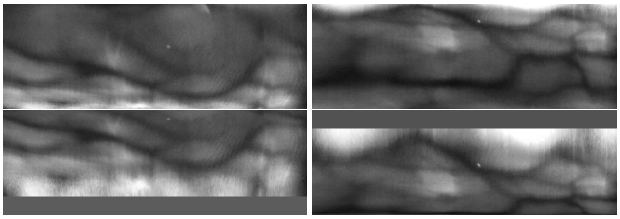

Figure 7. Finger samples exhibiting a large rotational distance (PLUSVein-FR: subjectId 50, fingerId 4, sampleNo 1, rotation angle $\pm 45°$). Top: acquired image, bottom: rotation corrected images.

The second data set, PLUSVein-FR-ND, consists of finger vein images which rotation angles are normally distributed over the range of $\pm 45°$ and should correspond to a realistic scenario. The rotation contained is a lot less than for PLUSVein-FR-ED. The EER for the original data set is 3.39%. EPN improves the EER to 1.72%, CPN to 1.52%, the fixed angle approach to 0.66% and the fixed angle correction to 1.13%, respectively. The different MPE scenarios again improve the performance. The best MPE res-

Data Set	Method	EER (CI)	FMR100	FMR1000	ZeroFMR	RPD	RPI
PLUSVein-FR-ED	No Correction	21.63 (± 1.01)	38.69	46.18	58.06	-	-
	CPN	15.34 (± 0.88)	23.89	28.73	40.88	-	41.0
	EPN	15.87 (± 0.89)	25.61	31.39	42.60	-	36.3
	Fixed Angle ($\varphi = 20°$)	5.24 (± 0.30)	7.00	8.85	12.97	-	312.5
	Known Angle	5.44 (± 0.55)	9.49	14.66	22.63	-	297.6
	MPE 2 Cameras	1.66 (± 0.31)	1.86	2.86	5.92	-	1202.8
	MPE 3 Cameras	1.13 (± 0.26)	1.13	1.60	3.13	-	1807.1
	MPE 4 Cameras	0.60 (± 0.19)	0.53	1.00	3.20	-	3513.8
	MPE 7 Cameras	0.33 (± 0.14)	0.20	0.87	2.07	-	6379.3
	PCT 15°	3.00 (± 0.42)	4.21	7.48	21.23	-	620.3
	PCT 30°	3.53 (± 0.45)	4.53	7.26	16.39	-	512.2
	PCT 45°	3.91 (± 0.48)	6.12	10.70	24.87	-	452.9
PLUSVein-FR-ND	No Correction	3.39 (± 0.44)	5.31	7.49	16.58	-	-
	CPN	1.52 (± 0.30)	1.72	2.32	5.37	-	122.3
	EPN	1.72 (± 0.32)	1.86	2.59	5.70	-	96.4
	Fixed Angle ($\varphi = 20°$)	0.66 (± 0.11)	0.60	1.05	1.48	-	412.4
	Known Angle	1.13 (± 0.26)	1.19	2.45	3.78	-	200.4
	MPE 2 Cameras	0.80 (± 0.22)	0.80	1.26	2.86	-	324.0
	MPE 3 Cameras	0.53 (± 0.18)	0.40	0.73	1.20	-	534.1
	MPE 4 Cameras	0.67 (± 0.20)	0.60	0.93	1.87	-	407.3
	MPE 7 Cameras	0.34 (± 0.14)	0.20	0.53	1.00	-	909.9
	PCT 15°	2.20 (± 0.36)	2.74	4.61	13.03	-	53.7
	PCT 30°	2.72 (± 0.40)	3.54	4.60	12.14	-	24.7
	PCT 45°	2.80 (± 0.40)	3.79	6.59	18.58	-	21.0

Table 2. Comparison of evaluated rotation compensation schemes.

ult is achieved for the 7 camera scenario hitting an EER of 0.34% which corresponds to an RPI of 910%. The PCT approach improves the recognition performance compared to the original data set as well, but not to the same extent as the other methods. The best PCT result is achieved with an EER of 2.20% for a rotational distance of 15° between the perspectives used for the PCT generation. Reasons for the lesser improvement compared to the other methods are: (1) According to [11], the other methods can handle small rotation better than larger rotations whereas PCT keeps the recognition performance quite stable over the whole range under investigation. (2) The single perspective templates used for the PCT generation contain less details than the templates used for the other approaches.

7. Conclusion

In this article, we proposed two novel methods for rotation invariant finger vein recognition. The first method, multi perspective enrolment, utilizes multiple finger vein images acquired during enrolment and compares, just as for commonly used finger vein recognition systems, a single perspective during authentication. The second method, perspective cumulative finger vein templates, combine multiple finger vein images from different perspectives into one larger template that holds the vein information over the whole range of interest. Additionally, we introduced two publicly available data sets, PLUSVein-FR-ED and PLUSVein-FR-ND, which were especially designed for the analysis of robustness of finger vein recognition systems against longitudinal finger rotation.

Both methods increase the recognition performance compared to the original data set without applying any rotation correction or compensation method. MPE achieves superior results with respect to all other rotation tolerant schemes. If enough cameras are used during enrolment, negative effects of longitudinal finger rotation on the recognition performance can be inhibited. PCT still has some issues, mainly related to the generation of the template. In order to achieve satisfactory results for the template generation, the degree of detail of the vein pattern had to be reduced. This inevitably leads to worse recognition rates. For both methods, the improvement of the recognition performance is achieved by increasing the effort (acquiring additional perspectives, template generation) during enrolment.

In our future work we will apply the PCT method not only in the feature space, but also in the image space. This would enable the possibility to use the proposed method not only on vein pattern based methods, but also on more sophisticated recognition systems as ASAVE [16] and DTFPM [8]. Also it might be possible to increase the level of detail in order to achieve better results. Additionally, we plan to further develop MPE in order that the number of required perspectives can be reduced. We also plan to evaluate the MPE approach for other recognition schemes than MC.

Acknowledgements

This work was supported in part by the European Union's Horizon 2020 Research and Innovation Program under Grant 700259, and in part by the FFG KIRAS Project AUTFingerATM under Grant 864785.

References

[1] Q. Chen, L. Yang, G. Yang, and Y. Yin. Geometric shape analysis based finger vein deformation detection and correction. *Neurocomputing*, 2018.

[2] B. Huang, Y. Dai, R. Li, D. Tang, and W. Li. Finger-vein authentication based on wide line detector and pattern normalization. In *Pattern Recognition (ICPR), 2010 20th International Conference on*, pages 1269–1272. IEEE, 2010.

[3] C. Kauba, B. Prommegger, and A. Uhl. The two sides of the finger - dorsal or palmar - which one is better in finger-vein recognition? In *Proceedings of the International Conference of the Biometrics Special Interest Group (BIOSIG'18)*, Darmstadt, Germany, 2018.

[4] A. Kumar and Y. Zhou. Human identification using finger images. *Image Processing, IEEE Transactions on*, 21(4):2228–2244, 2012.

[5] E. C. Lee, H. C. Lee, and K. R. Park. Finger vein recognition using minutia-based alignment and local binary pattern-based feature extraction. *International Journal of Imaging Systems and Technology*, 19(3):179–186, 2009.

[6] Y. Lu, S. J. Xie, S. Yoon, J. Yang, and D. S. Park. Robust finger vein roi localization based on flexible segmentation. *Sensors*, 13(11):14339–14366, 2013.

[7] D. Maio, D. Maltoni, R. Cappelli, J. L. Wayman, and A. K. Jain. FVC2004: Third Fingerprint Verification Competition. In *ICBA*, volume 3072 of *LNCS*, pages 1–7. Springer Verlag, 2004.

[8] Y. Matsuda, N. Miura, A. Nagasaka, H. Kiyomiu, and T. Miyatake. Finger-vein authentication based on deformation-tolerant feature-point matching. *Machine Vision and Applications*, 27(2):237–250, 2016.

[9] N. Miura, A. Nagasaka, and T. Miyatake. Feature extraction of finger-vein patterns based on repeated line tracking and its application to personal identification. *Machine Vision and Applications*, 15(4):194–203, 2004.

[10] N. Miura, A. Nagasaka, and T. Miyatake. Extraction of finger-vein patterns using maximum curvature points in image profiles. *IEICE transactions on information and systems*, 90(8):1185–1194, 2007.

[11] B. Prommegger, C. Kauba, M. Linortner, and A. Uhl. Longitudinal finger rotation - deformation detection and correction. *IEEE Transactions on Biometrics, Behavior, and Identity Science*, pages 1–17, 2019.

[12] B. Prommegger, C. Kauba, and A. Uhl. Longitudinal finger rotation - problems and effects in finger-vein recognition. In *Proceedings of the International Conference of the Biometrics Special Interest Group (BIOSIG'18)*, Darmstadt, Germany, 2018.

[13] B. Prommegger, C. Kauba, and A. Uhl. Multi-perspective finger-vein biometrics. In *Proceedings of the IEEE 9th International Conference on Biometrics: Theory, Applications, and Systems (BTAS2018)*, Los Angeles, California, USA, 2018.

[14] B. Prommegger, C. Kauba, and A. Uhl. On the extent of longitudinal finger rotation in publicly available finger vein data sets. In *Proceedings of the 12th IAPR/IEEE International Conference on Biometrics (ICB'19)*, pages 1–8, Crete, Greece, 2019.

[15] R. Veldhuis, L. Spreeuwers, B. Ton, and S. Rozendal. A high quality finger vein dataset collected using a custom designed capture device. In A. Uhl, C. Busch, S. Marcel, and R. Veldhuis, editors, *Handbook of Vascular Biometrics*, chapter 5, page 13 pages. Springer Science+Business Media, Boston, MA, USA, 2019.

[16] L. Yang, G. Yang, Y. Yin, and X. Xi. Finger vein recognition with anatomy structure analysis. *IEEE Transactions on Circuits and Systems for Video Technology*, pages 1–1, 2017.

[17] Y. Yin, L. Liu, and X. Sun. Sdumla-hmt: a multimodal biometric database. *Biometric Recognition*, pages 260–268, 2011.

[18] J. Zhang and J. Yang. Finger-vein image enhancement based on combination of gray-level grouping and circular gabor filter. In *Information Engineering and Computer Science, 2009. ICIECS 2009. International Conference on*, pages 1–4. IEEE, 2009.

[19] K. Zuiderveld. Contrast limited adaptive histogram equalization. In P. S. Heckbert, editor, *Graphics Gems IV*, pages 474–485. Morgan Kaufmann, 1994.